Massachusetts Institute of Technology

Functional Graphenic Materials via a Johnson-Claisen Rearrangement

By *Stefanie A. Sydlik* and *Timothy M. Swager**

[*]   Prof. Timothy M. Swager, Corresponding-Author, Stefanie A. Sydlik Author-Two
Massachusetts Institute of Technology, 18-597
Cambridge MA 02139 USA
E-mail: tswager@mit.edu

Current research in materials has devoted much attention to graphene, with a considerable

amount of the chemical manipulation going through the oxidized state of the material, known

as graphene oxide (GO). In this report, the hydroxyl functionalities in GO, the vast majority

that must be allylic alcohols, are subjected to Johnson-Claisen rearrangement conditions. In

these conditions, a [3, 3] sigmatropic rearrangement after reaction with triethyl orthoacetate

gives rise to an ester functional group, attached to the graphitic framework via a robust C-C

bond. This variation of the Claisen rearrangement offers an unprecedented versatility of

further functionalizations, while maintaining the desirable properties of unfunctionalized

graphene. The resultant functional groups were found to withstand reductive treatments for

the deoxygenation of graphene sheets and a resumption of electronic conductivity is observed.

The ester groups are easily saponified to carboxylic acids *in situ* with basic conditions, to give

water-soluble graphene. The ester functionality can be further reacted as is, or the carboxylic

acid can easily be converted to the more reactive acid chloride. Subsequent amide formation

yields up to 1 amide in 15 graphene carbons and increases intergallery spacing up to 12.8 Å,

suggesting utility of this material in capacitors and in gas storage. Other functionalization

11111111114111

schemes, which include the installation of terminal alkynes and dipolar cycloadditions, allow for the synthesis of a highly positively charged, water-soluble graphene. The highly negatively and positively charged graphenes (zeta potentials of -75 mV and +56 mV, respectively), have been successfully used to build layer-by-layer (LBL) constructs.

1. Introduction

Chemically modified graphenes have captured the imagination of materials researchers and have a plethora of potential applications, ranging from polymer composites[1] to electronic devices[2] to biomedical devices,[3] which leverage the extraordinary mechanical, electronic, and thermal properties of graphene.[4] A significant emphasis has centered on the chemical manipulation of graphene oxide[5] (GO) through use of the high density of carboxylic acid, alcohol and epoxide functionality.[5- 8] Although GO is easy to manipulate synthetically, the material properties are inferior to graphene. The conductivity of graphene drops to that of an insulator upon oxidation to GO[9] and the effective elastic modulus drops by more than half.[10] To this end, researchers have developed methods to chemically reduce (deoxygenate) GO to restore the physical properties, including use of sodium borohydride,[9] hydrazine,[11, 12] vitamin C,[13] and thermal "reduction."[14- 16] However, significant drawbacks exist in that most of the functionalization methods developed for GO convert the surface bound hydroxyls and epoxides into carbon-heteroatom bonds[5, 7] that are heterolytically unstable and can be removed during reduction, allowing the reduced GO sheets to quickly assemble into stacked structures.

There are a number of advantages to graphene oxide functionalization schemes that install "reduction-proof" carbon-carbon bonds that allow the reduced GO to remain functionalized after reduction. In contrast to carbon nanotubes,[17, 18] GO can not be functionalized with strongly alkaline organometallic reagents, which produce hydroxide ions, due to the residual water, and cause a reduction of the GO.[19] The GO activation is important

because graphite is only functionalized peripherally and minimally exfoliated when functionalization is directly attempted.[20, 21] To extend GO functionalization schemes, our group has recently made use of the fact that most (if not all) of the hydroxyl functionalities are allylic alcohols that, if converted to vinyl-ethers, will undergo a [3, 3] sigmatropic Claisen rearrangement to produce reduced GO functionalized with tertiary amides.[22] Unfortunately, further chemical transformation of the tertiary amide was limited, so the utility of this method was not broad.

To expand the utility of this chemistry, we now report graphene functionalization by another variation of the Claisen reaction, known as the Johnson Claisen rearrangement.[23] In this process, triethyl orthoacetate is used as the solvent and reagent and in the presence of catalytic acid produces graphenes with ester functional groups. The resulting carbonyl groups are attached to the graphitic framework via a carbon-carbon bond that survives reductive graphene-deoxygenation conditions. This variation offers vast improvements over previous work in the the enhanced reactivity of the activated ester over the tertiary amide and opens doors for functional applications of this method. Furthermore, the cost of the reagents are considerably less. In this contribution, we demonstrate the efficacy of this process and the utility of the functional graphenes afforded by these methods.

2. Results and Discussion
2.1. Synthesis

GO was synthesized by a modified Hummers method.[24, 25] This synthesis uses highly oxidizing conditions and appropriate caution should be used in work-up/ manipulation to avoid exothermic thermal decomposition or reactions with oxidizable chemicals/ solvents. Moderately oxidized GO (C to O ratio of 3:1) was used for this procedure since it is amphiphilic, which allows for a better dispersion than fully oxidized GO in the organic conditions used. Fully oxidized GO (C to O ratio of ≤2:1) required significant sonication to

form a good dispersion in triethyl orthoacetate (TEOA) due to its hydrophilicity, while the

partially oxidized GO formed a good dispersion with only stirring. Both the lower oxidation

state and the minimalization of the sonication used in preparation allow for larger graphene

flakes and better electronic properties.

TEOA was chosen as the orthoacetate ester reagent and solvent for the reaction with

GO. While slightly more expensive than trimethyl orthoacetate, previous work suggested that

the higher boiling temperature of triethyl orthoacetate (108 $^{\circ}$C vs. 142 $^{\circ}$C) would be

advantageous to the extent of reaction.[22] Initial experiments confirmed the greater reactivity

of the ethyl ester. The use of the ethyl ester resulted in the greater intensity and clarity of the

new peaks in the infrared spectrum as well as a greater weight loss in the thermogravimetric

analysis (TGA), suggesting a higher density of ester groups installed. *para*-Toluene sulfonic

acid (TsOH) was chosen as the acid catalyst, and unexpected covalent incorporation of this

reagent would be readily apparent by the appearance of a sulfur peak in the X-ray

photoelectron spectroscopy (XPS) analysis. In our first generation of GO functionalization,

Cl-GO1 is produced by reaction in TEOA at reflux for 36 hours, followed by cooling to room

temperature, centrifugation, and washing with polar, aprotic organic solvents (tetrahydrofuran,

acetone) (**Scheme 1**).

Cl-GO1 was characterized by Fourier transform infrared spectroscopy (FTIR), TGA,

XRD, Raman spectroscopy, and X-ray photoelectron spectroscopy (XPS) and all are

consistent with the proposed transformation. The TGA showed a a similar total weight loss to

GO over the temperature range of 50 to 850 $^{\circ}$C, however, the decomposition profile shifts

such that weight loss predominantly occurred over one clean transition at 230 $^{\circ}$C, suggesting a

majority of one type of functional group. The temperature is near to where the decomposition

transition occurs in carbon nanotubes functionalized via C-C bonds.[18] To confirm that this

weight loss did not originate from reagent trapped in the interstitial gallery of GO, control

experiments were performed. GO was solicited in TEOA for 1 hour in the absence of the acid

catalyst. The dispersion was then centrifuged and some of the sample was taken wet, as well

as after drying under vacuum over night. TEOA is high boiling (boiling point of 142 ^{o}C), but

extremely volatile and from the wet sample, it can be observed that trapped TEOA is

completely released from the GO layers by 60 ^{o}C. Furthermore, after drying under vacuum,

the TGA trace of GO is unaltered from before the introduction to TEOA. This suggests that

TEOA does not react with GO without the acid catalyst, which offers further suggestion of the

proposed reaction. TsOH also can not the source of this weight loss or expansion since no

sulfur can be observed by XPS. (Figure S1)

The Raman spectra showed a slight decrease in the D-band at 1330 cm^{-1} of **Cl-GO1**

relative to GO and a general sharpening of the peaks, suggesting increased order. The XPS

spectra of **Cl-GO1** showed only carbon and oxygen peaks, although the carbon to oxygen

ratio had shifted from 3:1 (found in GO) to 4:1. Since a C to O ratio of 2:1 characterizes the

functional group itself, this represents a degree of thermal reduction as well as

functionalization in the reaction conditions. Furthermore, a high resolution scan of the carbon

peak showed that the C-O component peak at 286.5 eV decreased from 36% in **GO** to 26% of

the total carbon content in **Cl-GO1**. The C-C component peak at 284.7 eV increased from

52% in **GO** to 61% in **Cl-GO1**. Unfortunately, it is not possible to discern the sp^2 hybridized

C of the graphene lattice from the sp^3 hybridized C of the installed functional group in this C-

C component. However, this data can be interpreted that roughly 10% of the C-O bonds were

converted into C-C bonds, via reduction or functionalization. Additionally, the C=O

component at 287.3 eV decreases and the O-C=O at 288.8 eV increases and sharpens. All of

this is in accordance with the proposed transformation (Figure S2).[22, 26, 27]

The XRD spectra provide an analysis of surface functionalization and without surface

groups the reductively deoxygenated GO reassembles into stacked disordered graphite-like

structures (i.e. reduced GO in Figure 1). Pristine graphite has a regular interlayer spacing given by a sharp peak at 3.4 Å and with exfoliation to GO, this spacing becomes 8.49 Å. After reaction under the Johnson Claisen conditions, the peak defining the interlayer spacing cleanly expands to 9.93 Å, which suggests that functional groups were successfully and homogenously installed on the graphene surface **(Figure 1)**. This is slightly larger than the expansion to 9.3 Å that was observed for the installation of dimethylamide groups using the Eschenmoser Claisen reaction.[22] The interlayer spacing here might be expected to be larger given that use of the ethyl ester installs a group one carbon longer than *N,N*-dimethylacetamide dimethyl acetal used in the Eschenmoser Claisen reaction. It is also possible that the higher degree of functionalization by the present method contributes to this larger spacing.

Perhaps the most informative characterization of **Cl-GO1** comes from the FTIR spectra **(Figure 2)**. GO is characterized by several peaks including a broad, intense –OH stretch at 3425 cm^{-1}, a C-O stretch at 1075 cm^{-1}, and two C=O stretches at 1600 cm^{-1} (carboxylate) and 1735 cm^{-1} (peripheral lactones). In **Cl-GO1**, the –OH stretch is greatly decreased in relative intensity and a new peak appears at 2970 cm^{-1}. This latter peak is typical of the CH$_2$ asymmetric stretch of the methylene group, which would appear if the rearrangement occurs and a methylene spacer separates the functional group from the graphene network. The CH$_2$ of the ethyl group also contributes to this resonance. A new C-O peak also appears at 1240 cm^{-1}. Two sharp carbonyl peaks are visible at 1725 cm^{-1} and 1590 cm^{-1}. The C=O stretch at 1725 cm^{-1} is easily explained by the expected ethyl ester, however the shift of the carboxylic acid peak was not expected and merited further investigation. We find that the zeta potential of **Cl-GO1** after our organic solvent workup is -55mV at pH= 9, which is higher than GO saponified with base at the same pH (-38 mV). Given the ionizable nature of GO,[28] it is hypothesized that in the acid catalyst creates carbocations along the

basal plane of the GO, which activate the ester carbonyl. This facilitates the nucleophilic attack of water[5] liberated from the GO **(Figure 3)**.

Based on this finding, we endeavored to find conditions that would directly produce the carboxylic acid exclusively. Given the metastable intermediate, it seemed that favoring the formation of the carboxylic acid should be relatively straightforward. To this end, after the 36 hours at reflux, we treated the warm reaction mixture with 1M NaOH and allowed the reaction to stir an additional 3 hours as it cooled to room temperature. Then, the reaction mixture was centrifuged and washed with deionized water three times. The resultant material was suspended in DI water with the pH adjusted to 9.0 using NaOH to give a stable dispersion. This resulting material, **Cl-GO2**, now showed a zeta potential of -75 mV and a greater intensity of the carboxylate C=O at 1590 cm^{-1} in comparison to as-synthesized **Cl-GO1** (Figure S3). It is also noteworthy that the CH$_2$ stretching bonds are preserved in the IR spectra as would be expected for graphene-CH$_2$CO$_2$H groups.

Selectively trapping the ester by preventing the saponification proved to be more challenging. Introduction of sodium borohydride (NaBH$_4$), lithium aluminum hydride (LAH), and even bis-pyridinylidene (a powerful organic reducing agent),[29] either after or before the refluxing period did not prevent the formation of new carboxylates and measured zeta potentials of the products were approximately -60 mV.

2.1.1. Reduction of the Cl-GO

To test the robustness of the newly installed functional groups and to restore desirable electronic properties, we endeavored to reduce **Cl-GO1** using sodium borohydride. To this end, we used a well-established literature procedure to reduce GO,[9] using 20 mM NaBH$_4$ in THF (**Scheme 2**). Both the reduced GO (**red-GO**) and reduced **Cl-GO1** (**red-ClGO**) were characterized by TGA, Raman, FTIR, and XRD. The TGA shows a decreased weight loss for both species, as would be expected for the removal of the oxygen-based functional groups (Figure S4) and the Raman spectra showed a slight increase of the G band at 1575 cm^{-1} in

comparison with the D band at 1330 cm^{-1} (Figure S5). In **red-GO**, the FTIR spectrum shows

a significant decrease in intensity of the absorptions above baseline. Most notably, the

carbonyl peak at 1630 cm^{-1} decreases with respect to the peak at 1725 cm^{-1} and the peak at

1180 cm^{-1}, corresponding to C-O single bonds associated with residual oxygens bound to the

graphene, disappears. To contrast, **red-ClGO** still displays the characteristic C-H asymmetric

stretch of the methylene spacer at 2970 cm^{-1}, indicating that the installed functional group

remains intact. Furthermore, strong C=O stretches at 1570 and 1725 cm^{-1} remain, which is

expected since NaBH$_4$ should not reduce esters and carboxylic acids under these conditions.

Perhaps the most convincing piece of data can be found in the XRD spectrum. The spacing

remains expanded from the interlayer spacing of 8.49 Å found in GO with a sharp peak

indicating an interlayer distance of 9.71Å. This is slightly reduced from the 9.93 Å found for

Cl-GO1, but significantly distinct and expanded from the broad peak found over the spacings

of 3.4- 5.5 Å characteristic of reduced GO[9] (Figure 1).

The most important test of the effectiveness of our functionalization and reduction

scheme comes with the determination of the electronic properties, most notably electrical

conductivity. In attaining processability, often the sought-after electronic properties of

functionalized graphenes can be lost. Functional groups create sp^3 hybridized defects that tend

to disrupt the delocalized electronic structure. However, the functional groups also enhance

the solubility and prevent aggregation, which could allow oxygen-based defects to be

removed more completely with chemical reduction. Electrical conductivities were determined

by a 4-point probe. Pristine single-layered graphene is an impressive conductor[4] ($\sigma > 10^8$

S/m) and the aggregation into graphite reduces the conductivity to 10^3-10^7 S/m, which is still

considered highly conductive.[28] GO is accepted to be an insulator and chemical reduction of

GO only partially restores the electronic properties.[9] To compare to these systems, the

conductivity of **Cl-GO1** and **red-ClGO** were compared to the standard systems (**Table 1**). It

is observed that although GO is an insulator, **Cl-GO1** does show low conductivity, presumably due to partial reduction during the reaction by liberated alcohol groups.[30] Interestingly, **red-ClGO** reattains a greater degree of conductivity than is observed in **red-GO** using the same conditions, insinuating that the installed groups allow the restoration of some of the electronic delocalization. This suggests that GO functionalized this way may show promise for electronic applications or conductive composites.

2.1.2 Further Transformations

Having established the robust nature of the installed functional groups, we endeavored to further expand the utility of these methods. Considering the reactivity of the carbonyl groups installed, it is logical to evaluate reactions with amines to give functional amides. In a first strategy the amine was introduced directly to the ester/ carboxylic acid functionality in isolated **Cl-GO1** by allowing the reagents to stir overnight at 100 ^{o}C after sonication in dioxane solution. Three different bulky amines were investigated to achieve a further expansion of the graphene interlayer spacing **(Scheme 3).** Using increasingly bulky amines, the interlayer spacing, as measured by XRD, increased to 10.45, 10.65, and 12.4 Å. Following the same amidation procedure using GO instead of **Cl-GO1** results in materials with poorly ordered interlayer spacings. (Figure S6) The small difference in interlayer spacing with the biphenyl over the phenyl is understood to be a consequence of conformations that allow for the biphenyl to lay parallel to the graphene plane. The three dimensional nature of the triptycene, as expected, enforces a larger interlayer spacing. Materials with large interlayer spacings such as these show promise for use in capacitors or in gas storage applications.

Successful amidation was confirmed by a decrease in the intensity of the ester carbonyl at 1725 cm^{-1} and appearance of a new C=O peak at 1600 cm^{-1}, a frequency typical for amides (Figure S7). Successful incorporation of the nitrogen was confirmed using XPS. **Cl-GO1** is 80% C and 20% O, with no other elemental signals visible. XPS analysis of **AGO2** shows the emergence of a nitrogen peak, accounting for 1.5 % of the elemental

composition, with the balance of elements being carbon and oxygen. This translates to approximately 1 amide group per 30 graphene carbons, suggesting efficient functionalization over two steps.

Two additional amide functionalized GOs were synthesized to demonstrate the utility of this transformation for other applications. **AGO4** was synthesized as a substrate for further chemistry via the copper-based "Click" reaction[31] and **AGO5** is synthesized to give a water-soluble cationic graphene. To see if we could further increase the efficacy of this transformation, we chose to first transform some of the installed carbonyls to more-reactive acid chloride groups, and then carry out the amidation step. For this procedure, **Cl-GO2** (primarily carboxylic acid functionalities) was reacted with oxalyl chloride in dioxane in the presence of catalytic dimethyl formamide[32] to achieve acid-chloride functionalized GO (**AC-GO**). The presence of the acid chloride was confirmed by XPS and FTIR. XPS revealed a modest incorporation of 0.65% chlorine with a peak at 202 eV. This value is likely lower than the actually efficiency as the acid chloride easily reacts with humidity in the air during sample transfer to give carboxylic acids. The plausibility of this transformation is further suggested by an increased percentage of oxygen (24% in **AC-GO** vs. 20% in **Cl-GO1**). In the FTIR, the carbonyl peak was shifted to 1750 cm^{-1}, where a higher wavenumber suggests the covalent attachment to the more electron-withdrawing chloride group. Additionally, a sharp peak at 670 cm^{-1}, which can be attributed to the C-Cl, bond appears (Scheme S6).

These additional AGOs were characterized by FTIR and TGA to assure their covalent functionalization. Like AGO1-3, the C=O stretch was shifted to 1600 cm^{-1}, indicating amidation. The C-Cl peak at 670 cm^{-1} disappears. In **AGO4**, the weak stretch of the asymmetric CC triple bond appears at 2120 cm^{-1}. This peak was found to be greater in intensity that when the propargyl group was installed via direct amidation from **Cl-GO1**. Furthermore, XPS characterization of **AGO4** prepared from the acid chloride revealed a 4.9%

incorporation of nitrogen, suggesting an increase in functional group density to approximately 1 group per 15 graphene carbons. As a result of the greater density acheived, **AGO4** synthesized via the acid chloride, was used for further reactions. In **AGO5** the sp^3 umbrella stretches of methylene units intensify, as one would expect from the insertion of the *n*-propyl group. Additionally, the zeta potential at pH= 5.0, where the tertiary amide is protonated, was found to be +56 mV. This was an improvement on the zeta potential of +40 mV found in the **AGO5** synthesized from direct amidation of **Cl-GO1**.

2.1.2 Further Functionalizations using "Click" Chemisry

To further expand the usefulness of this chemistry, **AGO4** was subjected to a copper catalyzed 1,3-dipolar cycloaddition, or "Click" reaction of a termial alkyne and an azide. Given the popularity of this chemistry,[31, 33, 34] there are a wide variety of azides commercially available, thus adding significant chemical utility and versatility to this covalent functionalization of graphene. For purposes of demonstration, three different azides were selected. For the first example, an azide with a very characteristic elemental tag was selected so that the efficiency of the reaction could be quantified by XPS. To this end, sodium 3-azidopropane-1-sulfonate was synthesized by a simple literature procedure[35] and allowed to react at 50 ^{o}C in dioxane/ water overnight in the presence of copper catalyst to give **S-GO** (**Scheme 5**). **S-GO** was washed thoroughly and characterized by XPS, FTIR, and TGA to ensure successful functionalization. In the FTIR spectrum, the CC triple bond peak at 2120 cm^{-1} decreases greatly in intensity and the appearance of a sharp peak 1340 cm^{-1} suggests the presence of the sulfonate, while the other distinct peaks of a sulfonate at around 1150 and 1000 cm^{-1} are blended with other signals found in Cl-GO (Figure S8). Further proof of successful functionalization can be drawn from the XPS, which shows a sulfur peak at 153 eV. The elemental composition is shown to be 80% C, 14% O, 5% N and 1% S, suggesting that approximately 1 in 40 graphene carbons have a "Click" functional group.

To ensure that this procedure could be applied to other azides, easily prepared azidomethanol[33] and commercially available methoxypolyethylene glycol azide (PEG-azide) were subjected to the same conditions to give **PEG-GO** and **HO-GO**. PEG was chosen due to its versatility and the suggested potential of **Cl-GO** as a route to polymer-grafted graphene for use in composite materials. These materials were characterized by TGA and FTIR. Sucessful incorporation in **PEG-GO** was identifiable in the FTIR spectrum by the diminution of the CC triple bond stretch at 2120 cm^{-1}, strengthening of the methylene CH$_2$ asymmetric stretch signals at 2970 cm^{-1} and the appearance of new C-O peaks in the 1100 to 1300 cm^{-1} region.

Similarly, an increase in the intensity of the OH stretch at 3500 cm^{-1} was observed for **HO-GO** (Figure S8). All three materials prepared by "Click" chemistry show increased weight loss in their TGA and water solubility, which further confirms the characterization. Highly negatively charged graphene is readily available, considering that oxidation to graphene oxide gives many negatively charged groups. Overcoming these negatively charged groups with a reaction that installs a significant amount of positively charged groups is often a challenge,[6] however it was easily overcome with the functionalization method used to produce **AGO5**. To demonstrate the efficacy of this chemistry in producing stable, charged suspensions in water, we chose to construct layer-by-layer (LBL) films. Here we demonstrate the assembly of both alternating polymer- graphene and all graphene LBL assemblies.

Graphene solutions were prepared at a concentraion of 0.5 mg/mL in deionized (DI) water and the pH was adjusted using aqueous hydrochloric acid (HCl) or sodium hydroxide. The cationic graphene solution, **AGO5**, was adjusted to pH= 5.0, where the zeta potential is +56 mV and the anionic graphene solution, **Cl-GO2**, was adjusted to pH= 9.0, where the zeta potential is -75 mV. It is important to note that the zeta potential of GO at this pH is only -30 mV.[6] This significant increase in zeta potential eases the LBL process and opens doors for further applications in LBL assemblies. Polymer solutions of cationic polyallylamine

hydrochloride (PAH) and anionic polystyrene sulfonate (PSS) were prepared at a

concentration of 10 mM and adjusted to pHs of 4.0 and 8.0 respectively, using aqueous HCl

or NaOH. Glass slides were treated with a plasma/ ozone surface treatment, which leaves the

glass negatively charged.

To begin, the charged graphene solutions were alternated with well-known charged

polymers. To ensure a uniformly charged substrate, the plasma treated glass was first dipped

in a PAH solution for 20 minutes. To build the LBL film, substrates were subsequently

dipped in either anionic **Cl-GO2** or PSS for 20 minutes, dried using a gentle nitrogen stream,

dipped in PAH or cationic **AGO5** for 20 minutes and dried using a gentle nitrogen stream.

Since the polymers absorb minimally in the visible region, the UV-Vis spectra was taken only

after each bilayer of graphene-polymer was built to monitor the LBL growth. Using these

conditions, the LBL films were grown up to 8 bilayers. Using the absorbances at 350 nm and

500 nm, it was observed that the UV-Vis spectra intensity increased linearly with the

application of each bilayer, confirming well-behaved, uniform growth (**Figure 4**).

Confident in the ability of the charged graphene solutions to form hybrid LBL

constructs, we endeavored to extend these conditions to make an all graphene film. Starting

with a layer of PAH to assure good adhesion, a LBL film 12 layers thick was assembled using

the same procedure that was effective for the hybrid constructs. Here, the UV-Vis spectrum

was taken after each layer (**Figure 5a**). The cationic layers of **AGO5** absorbed slightly more

than the anionic. This can be explained by the larger graphene particles in the cationic

dispersion (1000 nm vs. 500 nm by light scattering), suggesting that there is a higher degree

of aggregation in that solution. This is intuitive since the absolute zeta potential is slightly

lower, the dispersion is by definition less stable. Additionally, it is observed that each

graphene layer of the all-graphene construct is much thicker than those adsorbed in the

polymer/ graphene hybrids. Presumably this is because in addition to the electrostatic

interactions that traditionally control LBL assembly, the π–π interactions of the graphene sheets also provide favorable energetics for adsorption. Like the polymer/ graphene hybrids, the absorbance intensity at 350 and 500 nm is plotted and fit to a line (**Figure 5b**).

3. Conclusions

In this report, the hydroxyl functionalities in GO were considered allylic alcohols and subjected to Johnson-Claisen rearrangement conditions to give esters and carboxylic acids connected to the graphene basal plane via a "reduction-proof" carbon-carbon bond that survives conditions used to further deoxygenate the graphene surface. The ability of this functional group to withstand reduction is demonstrated and a resumption of electronic conductivity greater than that found in pristine reduced GO is measured. The ester groups are easily saponified to carboxylic acids *in situ* with basic conditions, to give negatively charged water-soluble graphene (**Cl-GO2**). The ester functionality can be further reacted as is, or the carboxylic acid can easily be converted to the more reactive acid chloride. To this end, we have appended several different amines of varying utility through an amide formation (up to 1 in 15 carbons by XPS). **AGO1-3** allow for an increase in the intergallery spacing up to 12.8 Å, suggesting utility of this material in capacitors and in gas storage. **AGO4** proves an adequate substrate for further functionalization using "Click" chemistry. The high density of carboxylic acid groups give highly negatively charged, water soluble graphene and tertiary-amine functionalized **AGO5** gives a complementary highly positively charged graphene (zeta potentials of -75 mV and +56 mV, respectively). These highly charged graphenes have been successfully used to build layer-by-layer (LBL) constructs with either oppositely charged polymers or in an all-graphene construct. This variation of the Claisen rearrangement offers improvements over previous work in the cost of reagents as well as the ease and versatility of further functionalizations. Applications of these functional graphene derivatives are diverse and are in the process of be being further explored.

4. Experimental

4.1 Materials

Triethyl orthoacetate and dioxane were passed through a column of activated alumina to eliminate moisture before use in reactions. Anhydrous tetrahydrofuran was collected from an Innovative Technology purification system. Graphite powder (99%, synthetic, 325 mesh) was used as received from Sigma Aldrich. All other chemicals used for synthesis were of reagent grade and used as received from Sigma-Aldrich. All synthetic reactions were carried out under an inert atmosphere of argon unless otherwise noted.

4.2 Instrumentation

Fourier transform infrared spectroscopy (FTIR) spectra were determined using a Nexus Model 470/670/870 Spectrophotometer using the Omnic software package. Thermogravimetric analysis (TGA) was performed using a TA Instruments Q50 under nitrogen at a scan rate of 15°C/ min from 50 °C to 850 °C. Raman spectra were taken on a Horiba Lab Ram with equipped with a 533 nm YAG laser using LabSpec 5 processing software. X-ray diffraction was measured using Cu Kα radiation on an Inel CPS 120 position-sensitive detector with a XRG 3000 generator using a 20-minute collection time. Zeta potentials were measured in water using a Brookhaven Instruments Corporation Phase Analysis Light Scattering (PALS) Zeta Potential Analyzer. All values are an average of 10 10-second scans. XPS spectra were recorded on a Kratos AXIS Ultra X-ray Photoelectron Spectrometer. Glass slides were prepared for LBL treatment using a Harrick PDC-32G Plasma Cleaner/ Sterilizer. The thickness of thin films were measured using a Dektak 6M stylus profiler by Vecco and electrical properties were measured utilizing a Signatone S-302-4 four point probe connected to a Keithley SCS-4200 source meter. Conductivities were calculated using the formula:

$\sigma = I / (V * t * 4.53)$, where I = current, V = voltage, t = film thickness, and 4.53 is the correction factor for the 4-point probe geometry.

4.3 Synthesis

4.3.1 Synthesis of Graphene Oxide (GO). Synthesis was accomplished using a modified Hummers method [25]. The product was lyophilized to yield 5.23g GO (68.18% C, 31.82% O) which was characterized by FTIR (Figure 1), TGA (Figure S1), XRD (Figure 2), Raman (Figure S3), and XPS (Figure S9).

4.3.2 Synthesis of reduced GO (redGO). A flame-dried 100 mL round bottomed flask was charged with 40 mg GO and 50 mL anhydrous tetrahydrofuran (THF). The reaction mixture was sonicated for 10 minutes to ensure good dispersion and then the flask was brought to 0 $^{\circ}$C in a ice water bath. Sodium borohydride (NaBH$_4$, 99%, 39 mg) was added in one shot and the reaction was allowed to warm to room temperature slowly over 5 hours. The reaction was then allowed to proceed at room temperature for an addition 8 hours. At this point, the reaction mixture was exposed to air and isopropanol (*i*PrOH) was slowly added to quench and NaBH$_4$ that had not yet reacted. Once bubbling ceased (addition of approximately 30 mL *i*PrOH), the reaction mixture was centrifuged (10 minutes at 11,000 rpm). The supernate was discarded and the residue was redispersed in *i*PrOH via vortex mixer and then centrifuged (10 minutes at 11,000 rpm). This process was repeated once more with *i*PrOH, twice with DI water, and once with acetone. The product was dried under vacuum overnight to yield 28 mg **red-GO** which was characterized by FTIR (Figure 1), TGA (Figure S1), XRD (Figure 2), and Raman (Figure S3). This procedure is adapted from Shin et al [9].

4.3.3 Synthesis of Claisen Graphene Oxide (Cl-GO). A flame-dried 500 mL round bottom flask was charged with GO (1.23g) and Triethyl orthoacetate (98%, 250 mL). The GO was dispersed via 10 minutes of bath sonication. Catalytic *para*-Toluene sulfonic acid (>97%, 21 mg) was added in one shot. The reaction vessel was placed in an oil bath and outfitted with a condenser column. The reaction was allowed to proceed at reflux (130° C) for 36 hours. This intermediate reaction mixture will be referred to as **Cl-GO**.

4.3.3 Purification of Cl-GO1. Reaction mixture **Cl-GO** was cooled to room temperature and centrifuged (10 minutes at 11,000 rpm). The supernate was discarded and the residue was redispersed in acetone via vortex mixer and then centrifuged (10 minutes at 11,000 rpm). This process was repeated four times with acetone. The product was dried under vacuum overnight to yield 1.08 g **Cl-GO1** (79.95% C, 20.41% O), which was characterized by FTIR (Figure 2), TGA (Figure S1), Raman (Figure S3), XRD (Figure 1), and XPS (Figure S10).

4.3.4 Purification of Cl-GO2. To favor the formation of carboxylic acid functional groups, at this point, 50 mL of 1 M sodium hydroxide was added. The reaction was allowed to cool to room temperature, while continuing to stir vigorously for an additional 3 hours. The reaction mixture was then centrifuged (10 minutes at 11,000 rpm) and the supernate was discarded. The residue was resuspended in deionized water using a vortex mixer and then centrifuged (10 minutes at 11,000 rpm) and the supernate discarded. This was repeated three times with water and twice with acetone. The remaining residue was dried under high vacuum to yield 1.15 g **Cl-GO2**, which was **Cl-GO1** by FTIR (Figure S1) and found to be water soluble with a Zeta potential of -75 mV at pH= 9.0.

4.3.5 Synthesis of reduced Cl-GO (redCl-GO). A flame-dried 100 mL round bottomed flask was charged with 40 mg **Cl-GO1** and 50 mL anhydrous tetrahydrofuran (THF). The reaction mixture was sonicated for 10 minutes to ensure good dispersion and then the flask was brought to 0 ^{o}C in a ice water bath. Sodium borohydride (NaBH$_4$, 99%, 39 mg) was added in one shot and the reaction was allowed to warm to room temperature slowly over 5 hours. The reaction was then allowed to proceed at room temperature for an addition 8 hours. At this point, the reaction mixture was exposed to air and isopropanol (*i*PrOH) was slowly added to quench and NaBH$_4$ that had not yet reacted. Once bubbling ceased (addition of approximately 30 mL *i*PrOH), the reaction mixture was centrifuged (10 minutes at 11,000 rpm). The supernate was discarded and the residue was redispersed in *i*PrOH via vortex mixer and then

centrifuged (10 minutes at 11,000 rpm). This process was repeated once more with *i*PrOH,

twice with DI water, and once with acetone. The product was dried under vacuum overnight

to yield 31 mg **red-ClGO** which was characterized by FTIR (Figure 1), TGA (Figure S1),

XRD (Figure 2), and Raman (Figure S3). This is the same procedure used to produce **red-GO**.

4.3.6 Synthesis of AGO1. A flame-dried 50 mL round bottomed flask was charged with 85 mg

Cl-GO1 and 25 mL dioxane. The reaction mixture was sonicated for 10 minutes to ensure

good dispersion and 1 mL Benzylamine (99%) was added in one shot. The reaction vessel

was warmed to 100 $^{\circ}$C in an oil bath and allowed to react overnight. After 12 hours, the

reaction mixture was allowed to cool to room temperature was centrifuged (10 minutes at

11,000 rpm). The supernate was discarded and the residue was redispersed in acetone via

vortex mixer and then centrifuged (10 minutes at 11,000 rpm). This process was repeated four

more times with acetone. The product was dried under vacuum overnight to yield 89 mg

AGO1 which was characterized by FTIR (Figure S5), TGA (Figure S7), and XRD (Figure

S4).

4.3.7 Synthesis of AGO2. Synthesis of **AGO2** was accomplished using the same method of

synthesis and purification as **AGO1** using 53 mg **Cl-GO1**, 25 mL dioxane, and 324 mg 4-

Phenylbenzylamine (97%). This yielded 60 mg **AGO2** (80.24% C, 18.83% O, 0.93% N by

survey) which was characterized by FTIR (Figure S5), TGA (Figure S7), XRD (Figure S4),

and XPS (Figure S11).

4.3.8 Synthesis of AGO3. Synthesis of **AGO3** was accomplished using the same method of

synthesis and purification as **AGO1** using 50 mg **Cl-GO1**, 25 mL dioxane, and 363 mg 2-

Aminotriptycene, which was synthesized using a literature procedure [36]. This yielded 63

mg **AGO3**, which was characterized by FTIR (Figure S5), TGA (Figure S7), and XRD

(Figure S4).

4.3.9 Synthesis of the acid chloride-GO (AC-GO). A flame-dried 100 mL round bottomed flask was charged with 256 mg **Cl-GO2**, 50 mL dioxane, and 5 drops dimethyl formamide. The reaction mixture was sonicated for 10 minutes to ensure good dispersion and 0.7 mL oxalyl chloride (99%) was added dropwise over 5 minutes. The bubbling started immediately and the reaction vessel was allowed to react overnight at room temperature. After 12 hours, the reaction mixture was centrifuged (10 minutes at 11,000 rpm). The supernate was discarded and the residue was redispersed in dichloromethane via vortex mixer and then centrifuged (10 minutes at 11,000 rpm). This process was repeated twice more with dichloromethane and and three more times with acetone. The product was dried under vacuum overnight to yield 118 mg **AC-GO** (75.63% C, 23.72% O, 0.65% Cl) which was characterized by FTIR (Figure S6), TGA (Figure S8), and XPS (Figure S12).

4.3.10 Synthesis of AGO4. A flame-dried 50 mL round bottomed flask was charged with 56 mg **AC-GO** and 25 mL dioxane. The reaction mixture was sonicated for 10 minutes to ensure good dispersion and 0.9 mL Propargylamine (>97%) was added in one shot. The reaction vessel was warmed to 100 $^{\circ}$C in an oil bath and allowed to react overnight. After 12 hours, the reaction mixture was allowed to cool to room temperature was centrifuged (10 minutes at 11,000 rpm). The supernate was discarded and the residue was redispersed in acetone via vortex mixer and then centrifuged (10 minutes at 11,000 rpm). This process was repeated twice with dioxane and twice more with acetone. The product was dried under vacuum overnight to yield 54 mg **AGO4** (84.86% C, 10.25% O, 4.89% N), which was characterized by FTIR (Figure S6), TGA (Figure S7), and XPS (Figure S13).

4.3.11 Synthesis of AGO5. Synthesis of **AGO5** was accomplished using the same method of synthesis and purification as **AGO4** using 53 mg **AC-GO**, 25 mL dioxane, and 1.0 mL 3(Dimethylamino)-1-propylamine (98%). This yielded 59 mg **AGO5**, which was

characterized by FTIR (Figure S6) and TGA (Figure S7). It was also found to be water-soluble with a Zeta potential of +56 mV at pH= 5.0.

4.3.12 Synthesis of S-GO. A flame-dried 25 mL round bottomed flask was charged with 15 mg **AGO4** and 12 mL 1:1 dioxane/ water. The reaction mixture was sonicated for 10 minutes to ensure good dispersion. Copper (II) sulfate (5 mg, 31 μmol), sodium ascorbate (2 mg, 10 μmol), and Sodium 3-azidopropane-1-sulfonate (100 mg, 0.53 mmol) were added in one shot and the reaction was allowed to stir at room temperature overnight. After 12 hours, the reaction mixture was centrifuged (10 minutes at 11,000 rpm). The supernate was discarded and the residue was redispersed in deionized water via vortex mixer and then centrifuged (10 minutes at 11,000 rpm). This process was repeated three times with DI water, twice with 1:1 acetone/ DI water, and once with acetone. The product was dried under vacuum overnight to yield 16 mg **S-GO** (80.82% C, 13.39% O 4.89% N, 0.9% S) that was characterized by FTIR (Figure S6), TGA (Figure S8), and XPS (Figure S14).

4.3.13 Synthesis of PEG-GO. The synthesis and purification of **PEG-GO** was completed using the same procedure as **S-GO** using 11 mg **AGO4**, 10 mL 1:1 dioxane/ water, 5 mg CuSO$_4$ (31 μmol), 2 mg sodium ascorbate (10 μmol), and 200 mg Methoxypolyethylene glycol azide (M$_n$= 2000, 0.1 mmol). The product was dried under vacuum overnight to yield 28 mg **PEG-GO** that was characterized by FTIR (Figure S6) and TGA (Figure S8).

4.3.14 Synthesis of HO-GO. The synthesis and purification of **HO-GO** was completed using the same procedure as **S-GO** using 25 mg **AGO4**, 20 mL 1:1 dioxane/ water, 8 mg CuSO$_4$ (50 μmol) and 4 mg sodium ascorbate (20 μmol). In this case, the azidomethanol was synthesized *in situ* from formaldehyde (0.1 mL, 37 wt% aqueous), glacial acetic acid (1 drop), and sodium azide (6.5 mg, 0.1 mmol) using a literature procedure [31]. The product was dried under vacuum overnight to yield 31 mg **HO-GO** that was characterized by FTIR (Figure S6) and

TGA (Figure S8). The rearrangement in the substitution of the triazole is indicated in Scheme S1.

Received: ((will be filled in by the editorial staff))
Revised: ((will be filled in by the editorial staff))
Published online: ((will be filled in by the editorial staff))

[1] Kim, H.; Abdala, A. A.; Macosko, C. W.; *Macromolecules*, **2010**, *43*, 6515- 6530.

[2] Di, C.; Wei, D.; Yu, G.; Liu, Y.; Guo, Y.; Zhu, D. *Adv. Mater.*, **2008**, *20*, 3289- 3293.

[3] Ang, P. K.; Ang, L.; Jaiwalt, M.; Wang, Y.; Hou, H. W.; Thong, J. T. L.; Lim, C. T.; Loh, K. P. *Nano. Lett.*, **2011**, *11*, 5240- 5246.

[4] Geim, A. K. *Science*, **2009**, *324*, 1530- 1534.

[5] Dreyer, D. R.; Park, P; Bielawski, C. W.; Ruoff, R. S. *Chem. Soc. Rev.*, **2010**, *39*, 228- 240.

[6] Park, J. S.; Cho, S. M.; Kim, W.-J.; Park, J.; Yoo, P. J. *ACS Appl. Mater. Interfaces*, **2011**, *3*, 360- 368.

[7] Subrahmanyam, K. S.; Ghosh, A.; Gomathi, A.; Govindaraj, A.; Rao, C. N. R. *Nanosci. and Nanotech. Lett.* **2009**, *1*, 28-31.

[8] Collins, W. R.; Schmois, E.; Swager, T. M. *Chem. Comm.,* **2011**, *47*, 8790- 8792.

[9] Shin, H.-J.; Kim, K. K.; Benayad, Q.; Yoon, S.-M.; Park, H. K.; Jung, I.-S.; Jin, M. H.; Jeong, H.-K.; Kim, J. M.; Choi, J.-Y.; Lee, Y. H. *Adv. Func. Mater.,* **2009**, *19*, 1987- 1992.

[10] Suk, J. W.; Piner, R. D.; An, J.; Ruoff, R. S. *ACS Nano*, **2010**, *4*, 6557- 6564.

[11] Becerril, H. A.; Mao, J.' Liu, Z.; Stolten, R. M.; Bao, Z.; Chen, Y. *ACS Nano*, **2008**, *2*, 463- 470.

[12] Eda, G.; Fanchini, G.; Chhowalla, M. *Nat. Nanotechnol*. **2008**, *3*, 270- 274.

[13] Fernandez-Merino, M. J.; Guardia, L.; Paredes, J.I.; Villar-Rodil, S.; Solis-Fernandez, P.; Matrinez-Alonso, A.; Tascon, J. M. D. *J. Phys. Chem. C*, **2010**, *114*, 6426- 6432.

[14] Schniepp, J. L.; Li, J.L.; McAllister, M. J.; Sai, H.; Herrera-Alonso, M.; Adamson, D. H.; Prud'homme, R.K.; Car, R.; Saville, D. A.; Aksay, I. A. *J. Phys. Chem. B*. **2006**, *110*, 8535- 8539.

[15] McAllister, M. J.; Li, J.-L.; Adamson, D. H.; Schniepp, H. C.; Abdala, A. A.; Liu, J.; Herrera-Alonso, M.; Milius, D. L.; Car, R.; Preud'homme, R. K.; Aksay, I. A. *Chem. Mater*. **2007**, *19*, 4396- 4404.

[16] Gao, X.; Jang, J.; Nagase, S. *J. Phys. Chem. C*, **2010**, *114*, 832- 842.

[17] Blake, R.; Gun'ko, Y. K.; Coleman, J.; Cadek, M; Fonseca, A.; Nagy, J. B.; Blau, W. J. *J. Am. Chem. Soc*. **2004**, *126*, 10226- 10227.

[18] Tasis, D.; Tagmatarchis, N.; Bianco, A.; Prato, M. *Chem. Rev*. **2006**, *106*, 1105- 1136.

[19] Fan, X.; Peng, W.; Li, Y.; Li, X.; Wang, S.; Xhang, G.; Zhang, F. *Adv. Mater.*, **2008**, *20*, 4490- 4493.

[20] Niyogi, S.; Bekyarova, E.; Itkis, M. E.; McWilliams, J. L.; Hamon, M. A.; Haddon, R. C. *J. Am. Chem. Soc.*, **2006**, *128*, 7720- 7721.

[21] Chakraborty, S.; Guo, W.; Hauge, R. H.; Billups, W. E. *Chem. Mater*. **2008**, *20*, 3134- 3136.

22222222222222222224222222

[22] Collins, W. R.; Lewandowski, W.; Schmois, E.; Walish, J.; Swager, T. M. *Angew. Chem. Int. Ed.,* **2011**, 50, 8848- 8852.

[23] Johnson, W. S.; Werthermann, L.; Bartlett, W. R.; Brocksom, T. J.; Li, T.-T.; Faulkner, D. J.; Petersen, M. R. *J. Am. Chem. Soc.*, **1970**, *92*, 741- 743.

[24] Hummers, W. S. and Offerman, R. E. *J. Am. Chem. Soc.* **1958**, *80*, 1339.

[25] Kovtyukhova, N I.; Ollivier, P. J.; Martin, B. R.; Mallouk, T. E.; Chizhik, S. A.; Buzaneva, E. V.; Gorchinskiy, A. D. *Chem. Mater.* **1999**, *11*, 771- 778.

[26] Yang, D.; Velamakanni, A.; Bozoklu, G.; Park, S.; Stroller, M.; Piner, R. D.; Stankovich, S.; Jung, I.; Field, D. A.; Ventrice, C. A. Jr.; Ruoff, R. S. *Carbon.* **2009**, *47*, 145-152.

[27] Murugan, A. V.; Muraliganth, T.; Manthiram, A. *Chem. Mater.* **2009**, *21*, 5004- 5006.

[28] Deprez, N.; McLachlan, D. S. *J. Phys. D: Appl. Phys.* **1998**, *21*, 101- 107.

[29] Murphy, J. A.; Garnier, J.; Park, S. R.; Schoenebeck, F.; Zhou, S.-z.; Turner, A. T. *Org. Lett.*, **2008**, *10*, 1227- 1230.

[30] Dreyer, D. R.; Murali, S.; Zhu, Y; Ruoff, R. S.; Bielawski, C. W. *J. Mater. Chem.* **2011**, *21*, 3443- 3447.

[31] Kolb, H. C.; Finn, M. G.; Sharpless, K. B. *Angew. Chem. Int. Ed.* 2001, 40, 2004- 2021.

[32] Lin, H.; Luengo, J. I.; Rivero, R. A.; Schulz, M. J.; Xie, R.; Zeng, J. WO2010/135504, A1 2010, 75-76.

[33] Kalisiak, J.; Sharpless, K. B.; Folkin, V. V. *Org.* Lett. **2008**, *10*, 3171- 3174.

[34] Iha, R. K.; Wooley, K. L.; Nyström, A. M.; Burke, D. J.; Kade, M. J.; Hawker, C. J. *Chem. Rev.* **2009**, *109*, 5620- 5686.

[35] Schnorr, J. M. and Swager, T. M. *J. Mater. Chem.* **2011**, *21*, 4768- 4770.

[36] Chong, J. H. and MacLachlan, M. J. *J. Org. Chem.* **2007**, *72*, 8683- 8690.
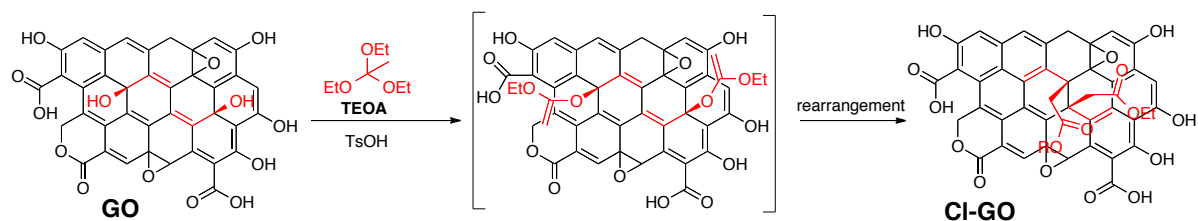
Scheme 1. Synthesis of Johnson-Claisen functionalized GO. **Cl-GO1** is the original material, functionalized with both carboxylic acids and esters. **Cl-GO2** is treated with strongly basic conditions in the work-up to give highly negatively charged, primarily carboxylate functionalized GO.
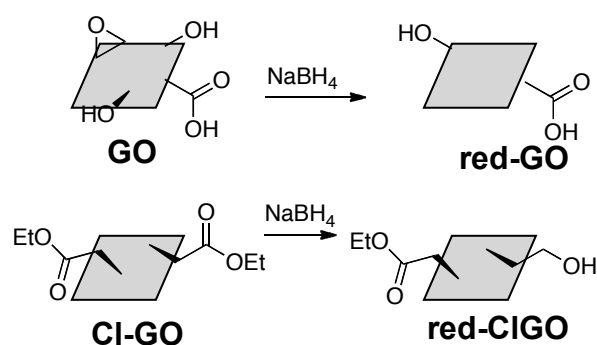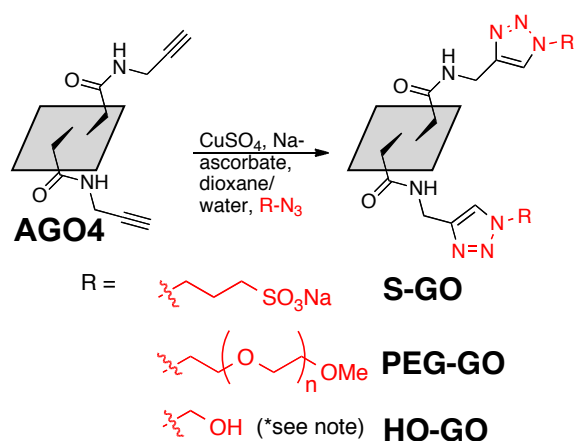

Scheme 2. Reduction of GO and **Cl-GO1** using $NaBH_4$. For clarity of the affected transformations, the intricacies of the graphene/ GO sheet were omitted.
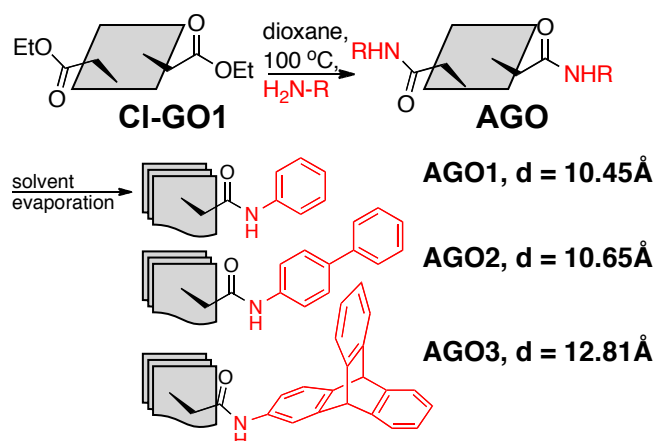
Scheme 3. Synthesis of AGO1-3 via direct amidation (Method 1) with interlayer spacings measured by XRD are included. For clarity of the affected transformations, the intricacies of the graphene/ GO sheet were omitted.
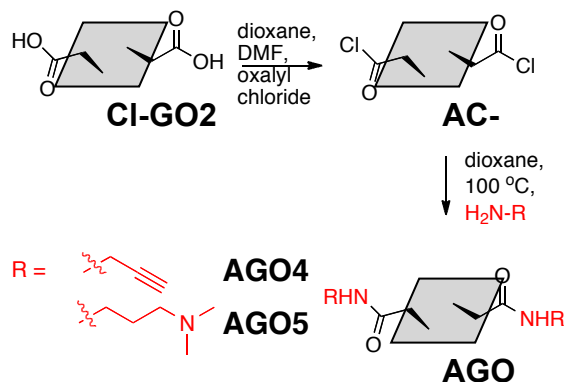
Scheme 4. Synthesis of AGO4-5 through the use of the acid chloride (Method 2). For clarity of the affected transformations, the intricacies of the graphene/ GO sheet were omitted.

Scheme 5. Functionalization of the Cl-GO using "Click" chemistry. HO-GO is synthesized from an in situ preparation of azido methanol, which results in a rearrangement of the substitution of the triazole ring.[33] Details can be found in Scheme S1. For clarity of the affected transformations, the intricacies of the graphene/ GO sheet were omitted.
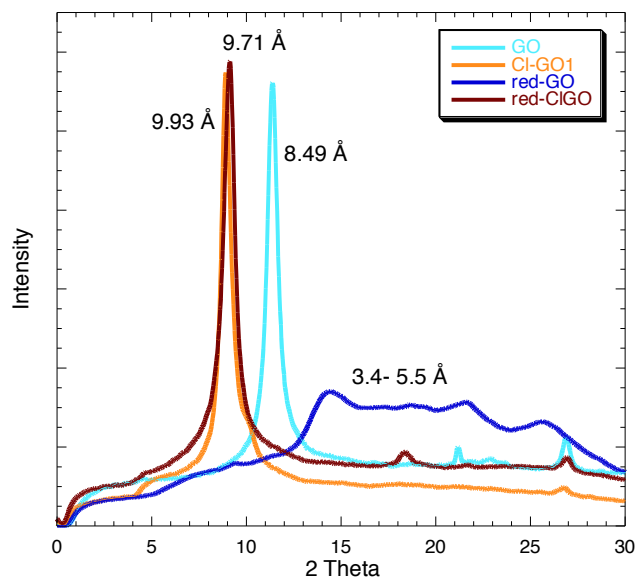
Figure 1. XRD spectra of GO, **Cl-GO1**, reduced GO (red-GO), and reduced Cl-GO1 (red-ClGO).
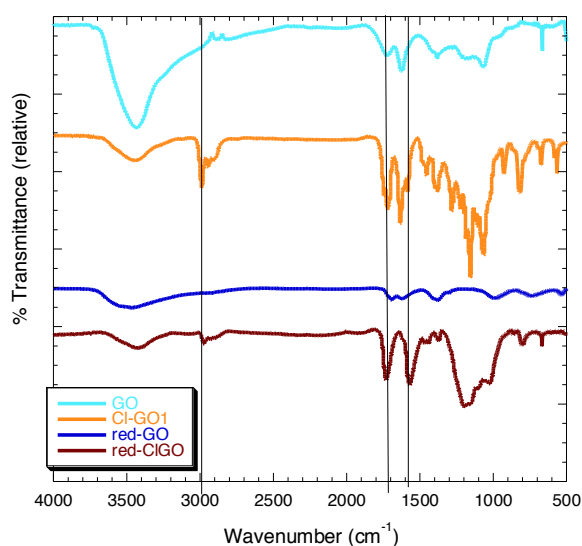

Figure 2. FTIR Spectra of GO, Cl-GO1, reduced GO (redGO), and reduced Cl-GO1 (red-ClGO). Spectra are off-set for clarity.
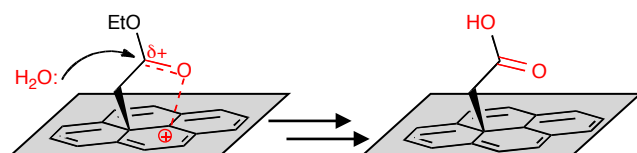

Figure 3. Schematic suggesting the activation and set-up of nucleophilic attack of the Claisen rearranged ester by residual water.
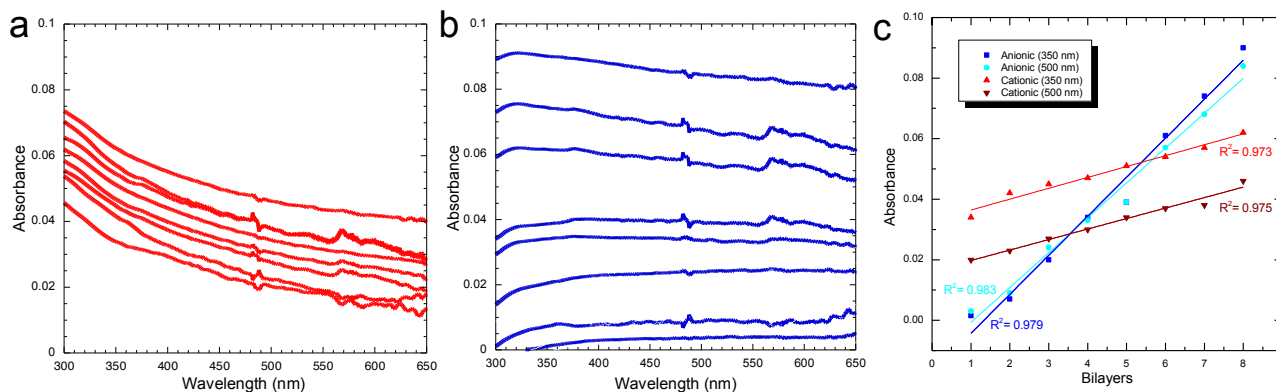
26262626262626262626264262626

Figure 4. UV-Vis absorbance of sequential layers of a) anionic graphene (**Cl-GO2**)/ PAH and b) cationic graphene (**AGO5**)/ PSS. c) Gives the linear fit of the UV-Vis absorbance at 350 and 500 nm. A detector change-over at 475 nm is responsible for the noise.
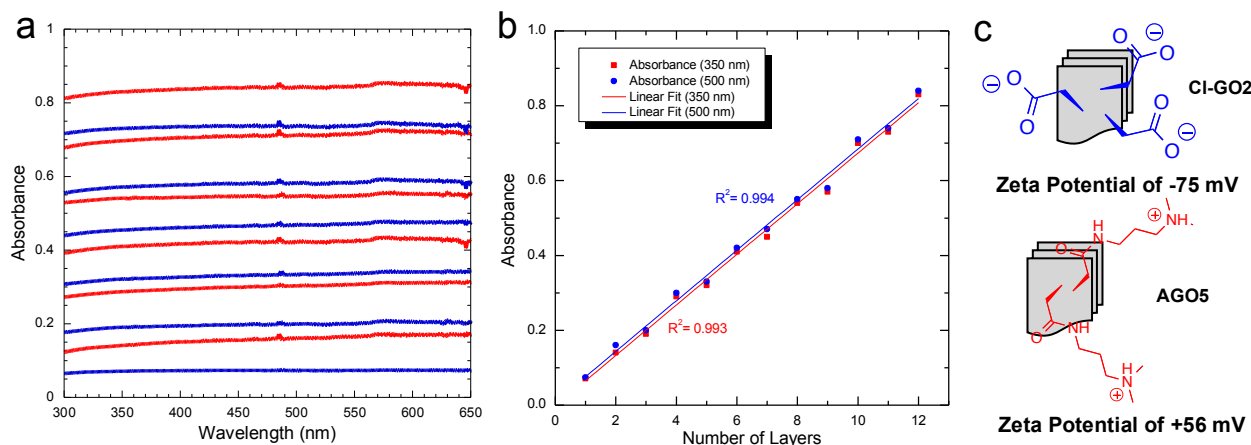

Figure 5. a) UV-Vis absorption data for the build-up of the all graphene LBL construct. Anionic layers are in blue and cationic layers are in red. A detector change-over at 475 nm is responsible for the noise. b) Linear fit for the absorbance at 350 and 500 nm. c) Representative structures of anionic (**Cl-GO2**) and cationic (**AGO5**) graphene and UV-Vis absorption data for the all-graphene LBL construct.

Table 1. Electronic conductivities and sheet resistances of graphite and related materials measured using a 4-point probe.
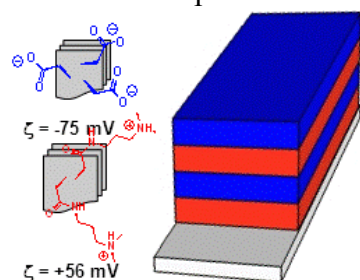
	Conductivity (S/m)	Sheet Resistance (kΩ/sq)
Graphite	1.1×10^5	10^{-5}
GO	1.2×10^{-7}	10^6
Cl-GO	1.0	80
red-GO	11	48
red-ClGO	39	1.6

The hydroxyl functionalities in graphene oxide (GO) are subjected to Johnson-Claisen rearrangement conditions, which trades the labile CO bond for a robust CC bond. Further functionalization allows for the synthesis of highly charged, water-soluble graphene. The negatively and positively charged graphenes (zeta potentials of -75 mV and +56 mV), have been successfully used to build layer-by-layer (LBL) constructs.

Keyword: Graphene

By Stefanie A. Sydlik and Timothy M. Swager*

Functional Graphenic Materials via a Johnson-Claisen Rearrangement

282828282828282828284282828

Supporting Information

Table of Contents

Scheme S1. Conditions for *in situ* prep of aziomethanol and rearranged triazole product.[31]
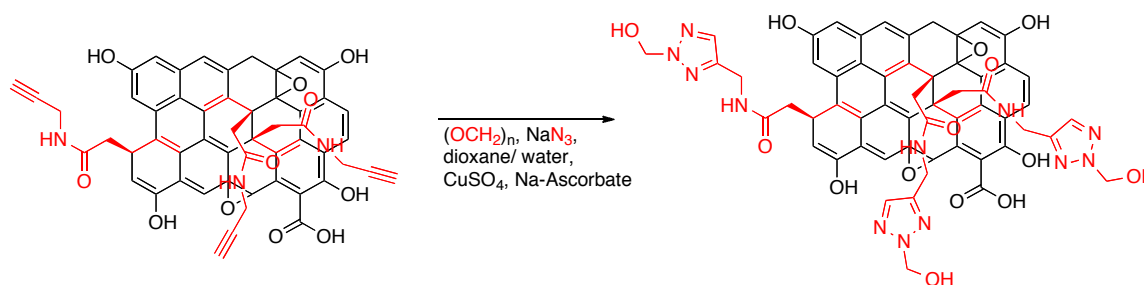
Figure S1. Thermogravimetric Analysis (TGA) curves from GO and GO treated with

TEOA (wet and after drying)
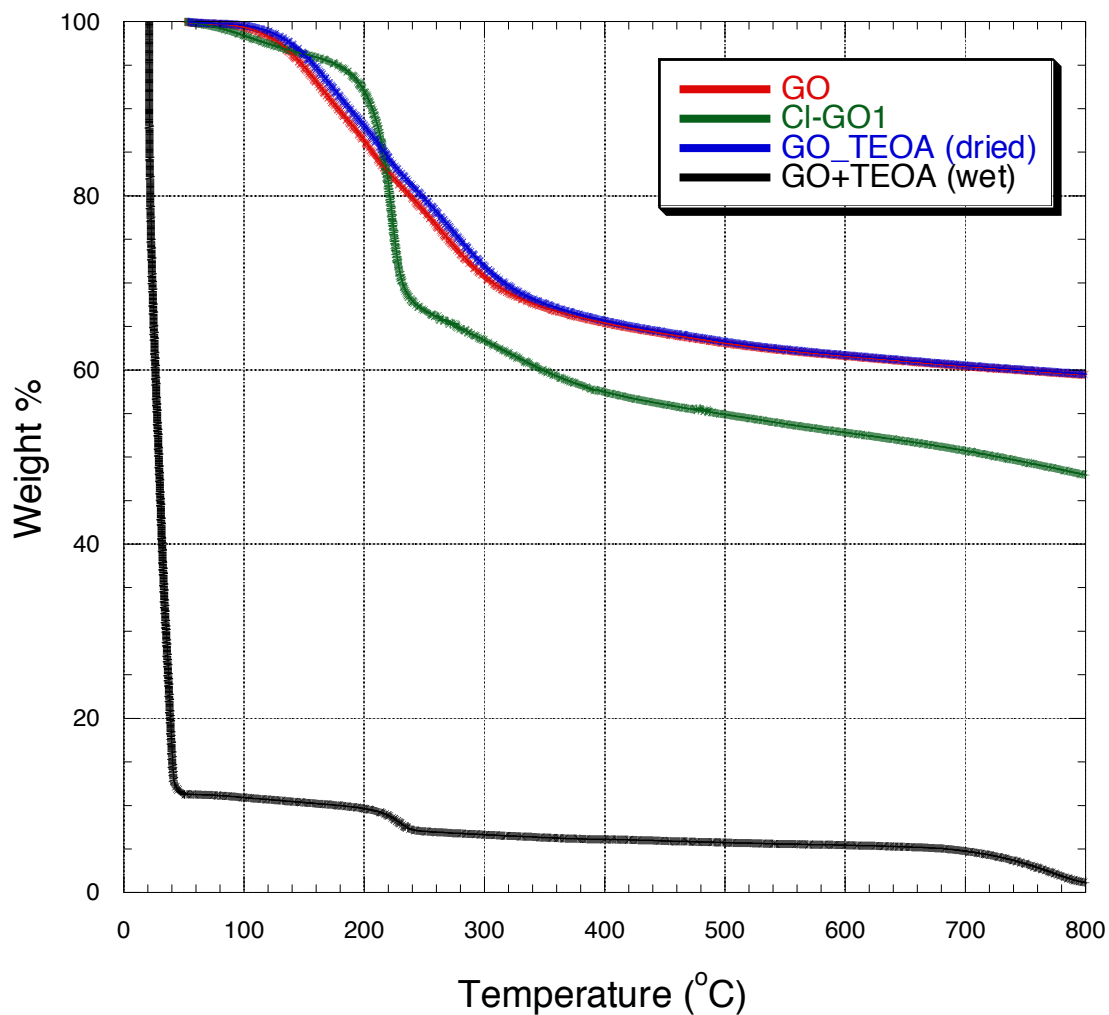
Figure S2. High Resolution X-ray photoelectron spectroscopy and fit curves for a) GO and

b) Cl-GO1

a) GO

b) Cl-GO1
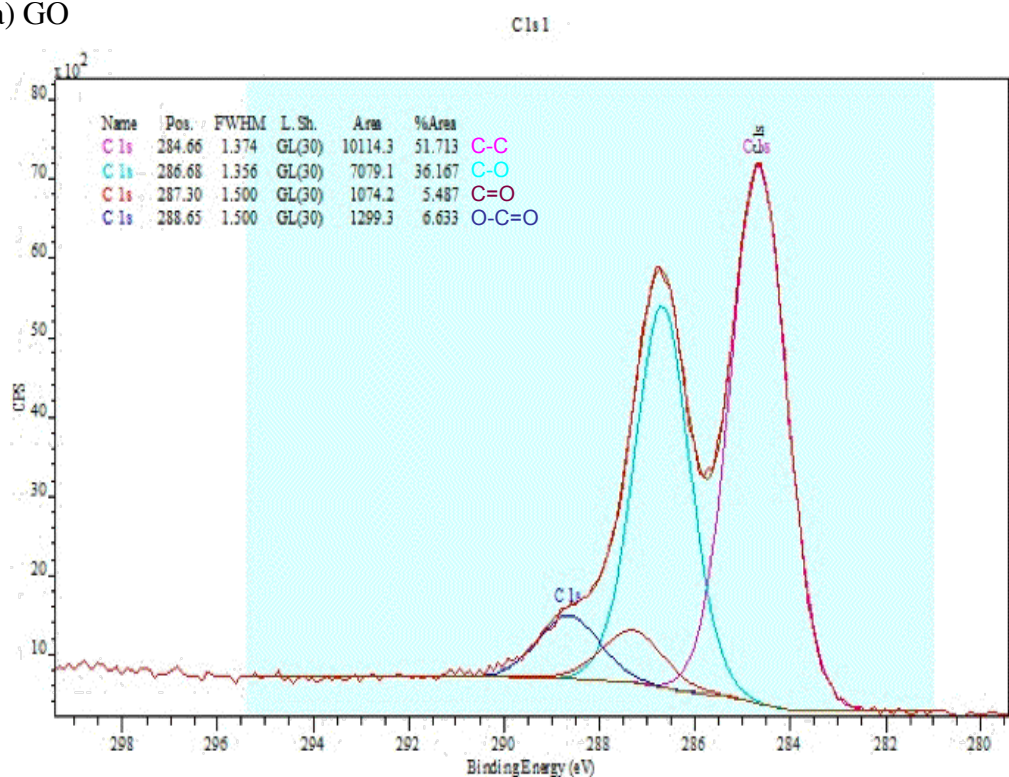
313131313131313131314313131
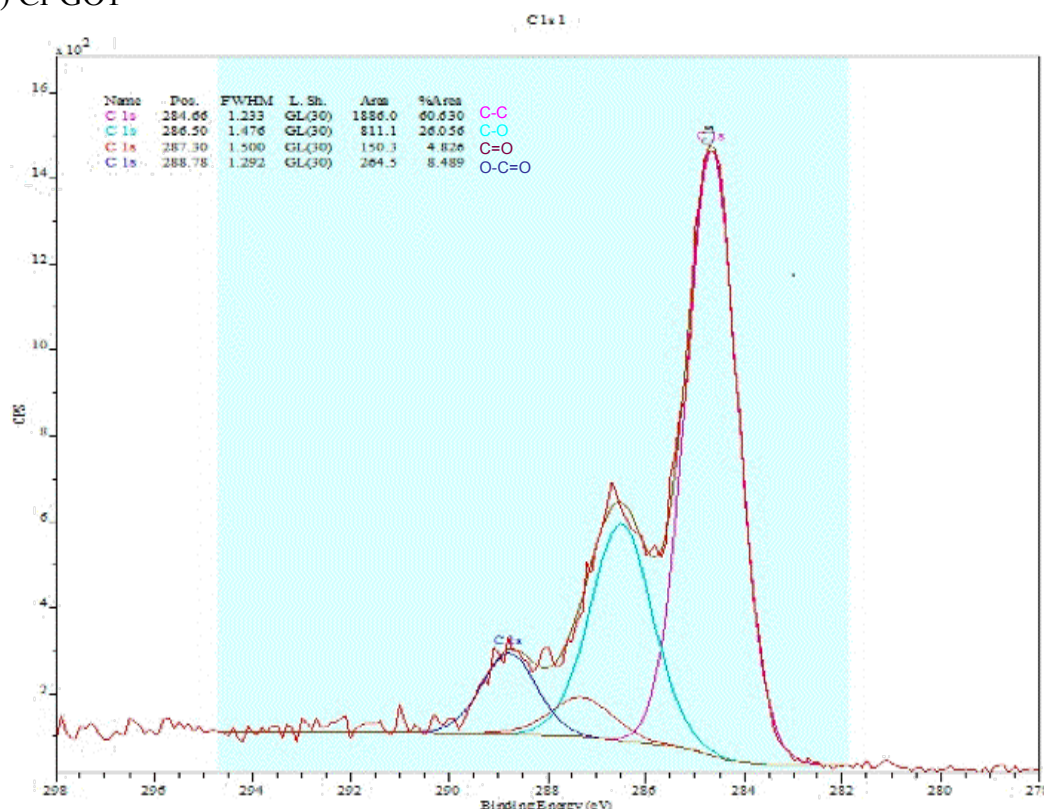
Figure S3. FTIR Spectra of Cl-GO2 in comparison with Cl-GO1. The intensity of the peakof

the carboxylate C=O peak (1590 cm^{-1}) in comparison with the ester C=O (1725 cm^{-1}) can be

observed.

Figure S4. Thermogravimetric analysis of GO, Cl-GO1, red-GO, red-ClGO.
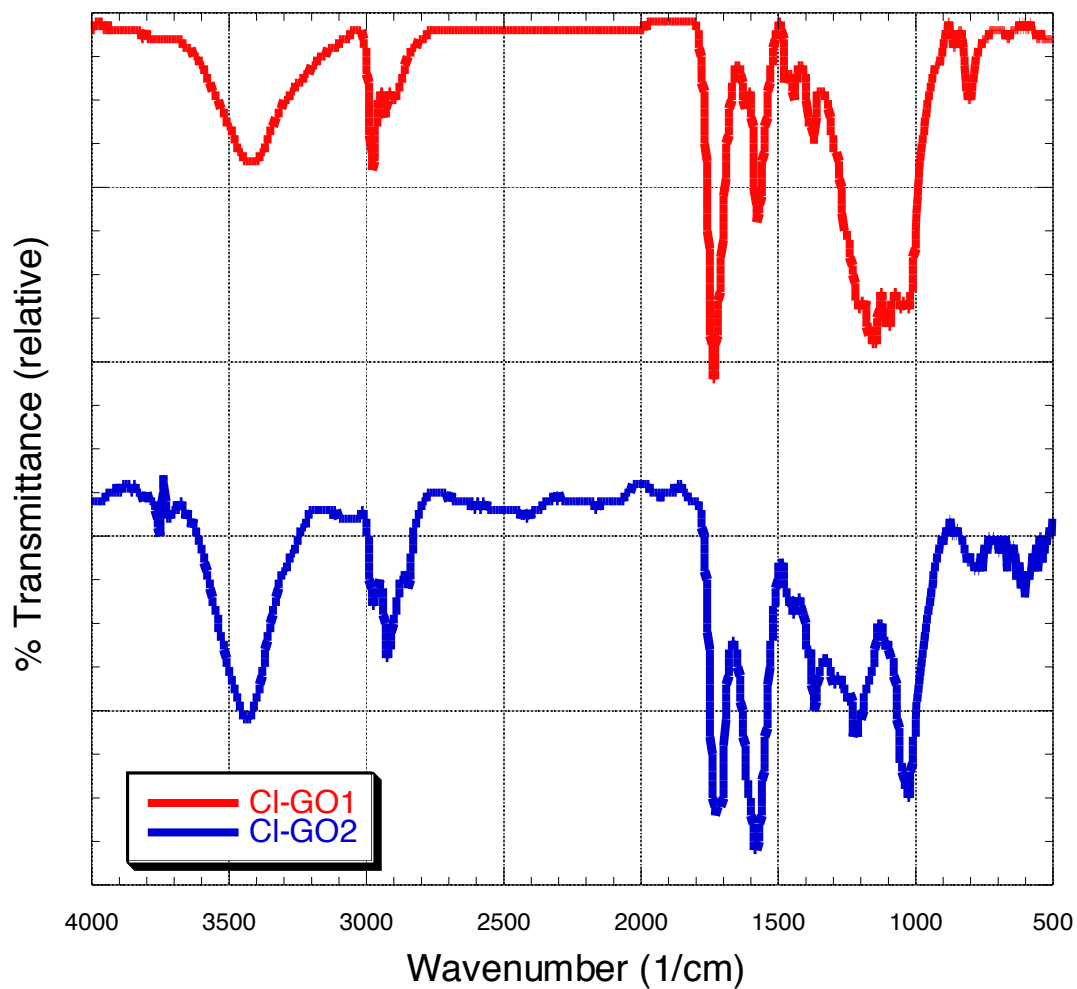
Figure S5. Raman Spectra of graphite, GO, Cl-GO, red-GO and red-ClGO. The y-axis is offset in each sample for clarity.

343434343434343434344343434

Figure S6a. X-ray diffraction patterns of AGO1-3. D-spacings are 10.45, 10.65, and 12.81 Å, respectively.

Figure S6b. X-ray diffraction patterns of GO treated with bulky amines (control).

Figure S7. FTIR spectra of AGO1-3 and AGO5.
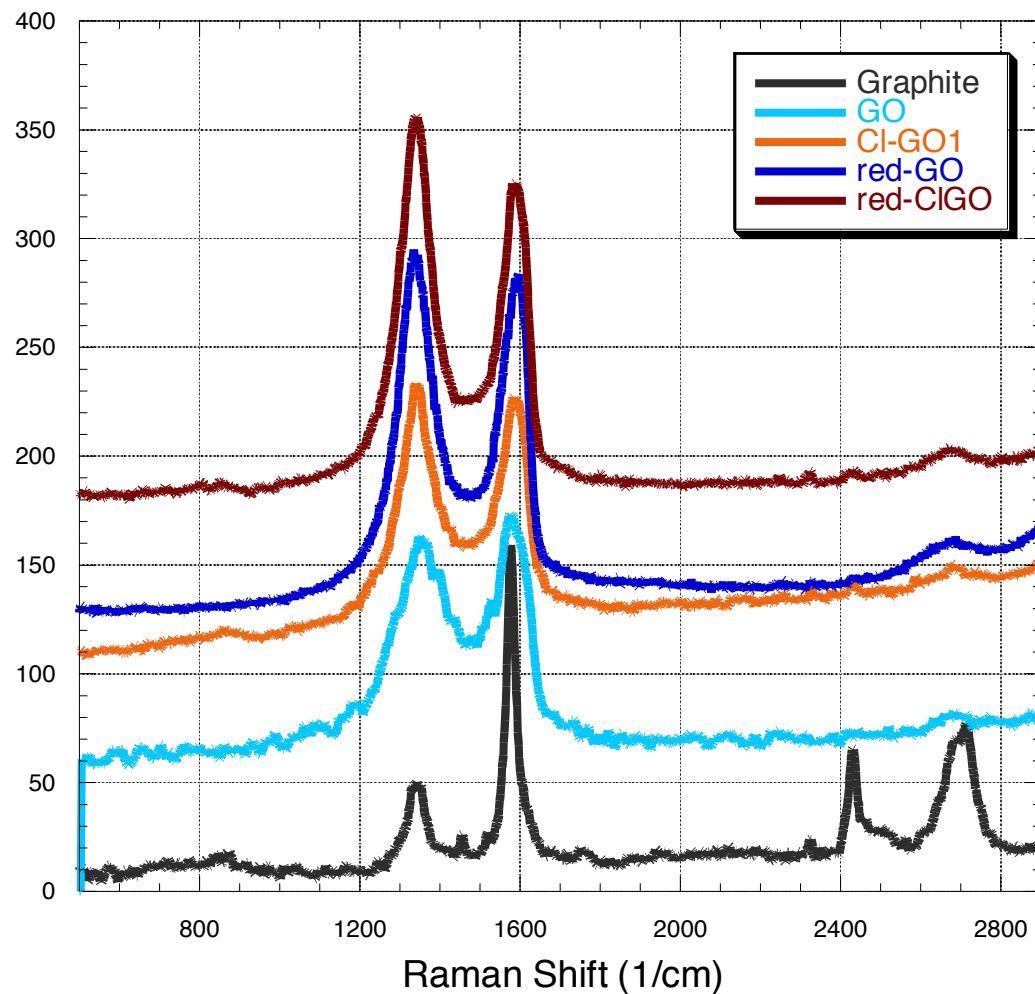
Figure S8. FTIR of the acid chloride, AGO4, SGO, PEG-GO, and HO-GO.

Figure S9. TGA of AGO1-5.

Figure S8. TGA of AC-GO, SGO, PEG-GO, HO-GO.
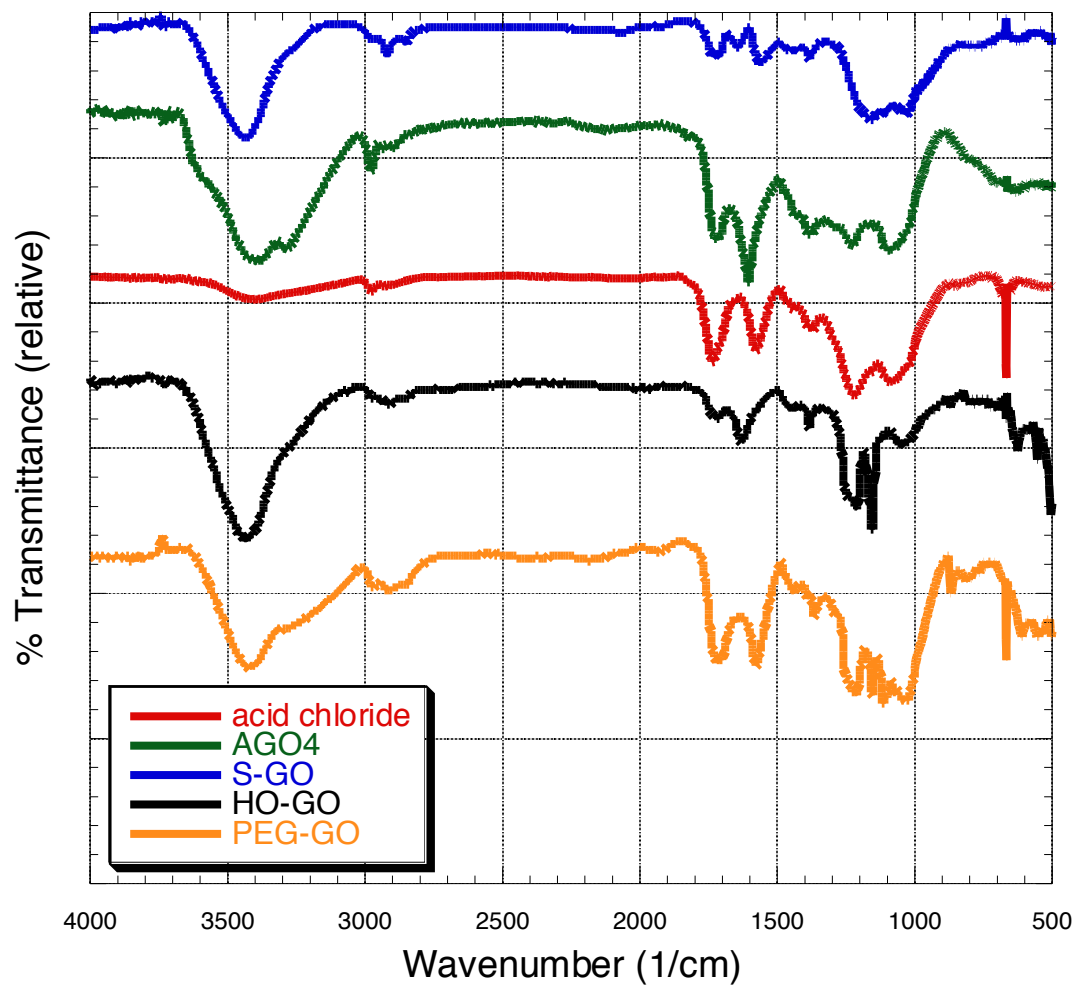
Figure S11. XPS Survey Data for GO.

```
--------------------------
```

Atomic Concentration Table

```
--------------------------
```

C1s	O1s	
0.314	0.733	RSF
58.873	137.529	CorrectedRSF
68.18	31.82	

yulin120307.107.spe: 6.ssgo		MIT CMSE
2012 Mar 7 Al mono 103.8 W 100.0 µ 45.0° 187.85 eV	8.8200e+004 max	3.44 min
Su1s/6: ssgo/1		

Atomic %
C1s 68.0
O1s 31.7
S2p   0.3

Figure S12. XPS Survey Data for Cl-GO1.

Quantification based on survey data (pass energy 160 eV, step size 1 eV)

Peak	Position BE (eV)	FWHM (eV)	Raw Area (CPS)	RSF	Atomic Mass	Atomic Conc	Weight%	Mass Conc %
C 1s	284.000	3.946	1131235.8	0.278	12.011	83.85		79.59
O 1s	532.000	3.286	864291.5	0.780	15.999	16.15		20.41

Figure S13. Survey and High-res XPS Data for AGO2.

Quantification Report: Survey

Peak	Position BE (eV)	FWHM (eV)	Raw Area (CPS)	RSF	Atomic Mass	Atomic Conc %	Mass Conc %
C 1s	284.000	3.538	1094729.0	0.278	12.011	84.31	80.24
O 1s	531.000	3.983	764857.4	0.780	15.999	14.85	18.83
N 1s	399.000	2.907	23072.0	0.477	14.007	0.84	0.93

Quantification Report: High-res
Quantification based on hires analysis (pass energy 20 eV, step size 0.1 eV)

Peak	Position BE (eV)	FWHM (eV)	Raw Area (CPS)	RSF	Atomic Mass	Atomic Conc %	Mass Conc %
C 1s	284.350	1.164	38776.8	0.278	12.011	98.72	98.51
N 1s	399.450	1.630	908.4	0.477	14.007	1.28	1.49

424242424242424242424424242

Figure S14. XPS Survey Data for AC-GO.

```
----------------------------
Atomic Concentration Table
----------------------------
     C1s       O1s       Cl2p
    0.314     0.733     0.954    RSF
   58.873    137.529   202.251   CorrectedRSF
    75.63     23.72      0.65
```

Figure S15. XPS Survey Data for AGO4.

```
--------------------------
Atomic Concentration Table
--------------------------
     C1s      N1s      O1s
    0.314    0.499    0.733    RSF
   58.873   93.593   137.529   CorrectedRSF
   84.86     4.89    10.25
```

Figure S16. XPS Survey Data for S-GO.

Atomic Concentration Table

C1s	N1s	O1s	S2p	
0.314	0.499	0.733	0.717	RSF
58.873	93.593	137.529	153.301	CorrectedRSF
80.82	4.89	13.39	0.90	